Journal of Engineering Research

Volume 7 | Issue 3 Article 57

2023

# Experimental and Theoretical Study on Reverse Osmosis Based Water Desalination

Amr M. Elbrol, Elsayed Elsaid, Yaser elsamadony, Farid A. Hammad, Khaled Khodary Ismaeil

Journal of Engineering Research (ERJ)
Vol. 7 – No. 3, 2023
©Tanta University, Faculty of Engineering
ISSN: 2356-9441 https://erjeng.journals.ekb.eg/ e ISSN: 2735-4873

# Experimental and Theoretical Study on Reverse Osmosis Based Water Desalination

Elsayed Ahmed[1], Y. A. F. EL-Samadony[1], Farid A. Hammad[1], Amr M. El-Brol[1], Khaled Khodary Ismaeil[1]

[1]Department of Mechanical Power Engineering, Faculty of Engineering, Tanta University, Egypt.

*Corresponding author email (Y.A.F.EL-Samadony@F-Eng.tanta.edu.eg)

***Abstract*- Freshwater availability has dropped due to population growth, inefficient use, climate change, and industrial pollution. Although the reverse osmosis, RO, system is one of the most effective desalination technologies worldwide, spiral wound membranes still need deeper theoretical and experimental investigations for removing salts under low energy consumption. In this study, the performance of a commercial pilot RO plant that utilizes a spiral wound seawater membrane module is experimentally investigated under a wide range of operating parameters. In addition, a Mathematical model is developed based on the solution-diffusion model theory and then solved using an in-house MATLAB algorithm to analyze its performance. The theoretical and experimental results were then compared. The present results revealed that the mathematical model's predictions were highly consistent with the actual experimental results, achieving an average accuracy of about 98%. The average deviation was 4.0578% when predicting water productivity and just 0.2755% when estimating the salt rejection coefficient. The findings of this study could assist designers in predicting the membrane's performance and selecting the most advantageous operational parameters for supplying water to the RO system.**

***Keywords*- Seawater desalination, (RO) reverse osmosis, The solution-diffusion model.**

## I. INTRODUCTION

The availability of fresh water has been dwindling in recent decades. While the supply of fresh water has remained relatively constant, the demand has surged due to the exponential growth of the population. The scarcity of fresh water can be attributed to inefficient utilization, the impacts of climate change, and contamination of water sources by industrial pollution. Over the past two decades, there has been a notable improvement in access to clean drinking water, thanks to global efforts aimed at enhancing sanitation and infrastructure.

To ensure sustained progress and uphold water security in the future, it is imperative to conduct further research into emerging sources of freshwater, such as desalinated seawater and treated wastewater. Presently, membrane technologies are the primary means of water treatment in desalination and wastewater reclamation processes. Although these methods have proven to be valuable and efficient, there remains an ongoing need to enhance and expand their capabilities. A basic understanding of the mechanisms that operate in membrane separation is essential to furthering the field. Transport models are the methodologies to understand membrane transport.

The standard requirement for the seawater desalination process, according to the WHO (World Health Organization), is the total dissolved solids concentration in fresh water (TDS) less than 600 mg/L is regarded as desirable, while lower numbers are typically preferable [1].

Thermal phase change technology for seawater desalination dominated the industry for the first 10 years of this century. On the other hand, the second decade has seen an increase in the use of desalination technology that uses membrane approaches [2], because thermal technology needs a lot more energy than membrane methods. The most well-known advantage of membrane technologies is that they consume far less energy than thermal technology, that's because the energy needs of RO stay at 3 to 4 (kW.hr/m3) for saltwater or drop to 0.5 to 2.5 (kW.hr/m3) for brackish water, whereas MSF requires between 10 and 16 (kW.hr/m3) and MED uses between 5.5 and 9 (kW.hr /m3) [3]. So reverse osmosis technology with the fastest growth rate in the world in desalination field.

The most popular membrane-based desalination technologies have been used to desalinate seawater, which is used for exclusion-controlled membrane filtering processes that run at low pressure, such as membrane distillation (MD), electrodialysis (ED), Nanofiltration (NF), and Forward Osmosis (FO), as well as diffusion- and size-exclusion-controlled processes that operate at high pressure, like Reverse Osmosis (RO).

The characteristics of various desalination membrane technologies are as follows. Electrodialysis is an electrochemical separation process that removes salt from the feed stream into a concentrated stream using selective ion exchange membranes and DC power. It uses between 1 and 12 kWh/m of energy. and provides the benefits of High salt removal and Reduced susceptibility to scale formation on the membrane. nevertheless Drawbacks: High capital costs, blockage, and energy loss.

Membrane distillation (MD) is a method for thermal separation in which phase change drives separation. Water vapor diffuses to the permeate side as a result of a difference in vapor pressures caused by a temperature differential across the membrane. It has the advantages of being able to handle elevated levels of salt concentration, having low fouling, and using low-temperature heat below 80 °C. while disadvantages include low water recovery and high energy consumption reach to (22–67 kWh/m).

Doi: 10.21608/ERJENG.2023.234375.1230

Journal of Engineering Research (ERJ)
Vol. 7 – No. 3, 2023
©Tanta University, Faculty of Engineering
ISSN: 2356-9441 https://erjeng.journals.ekb.eg/ e ISSN: 2735-4873

Nanofiltration (NF) is a membrane liquid-separation technology. That is similar to reverse osmosis (RO). NF offers strong rejection of multivalent ions, such as calcium, and poor rejection of monovalent ions, like chloride, in contrast to RO, which has great rejection of almost all dissolved solutes. NF is made from organic, thin-film composite membranes with a pore size range of 0.1 to 10nm, making it possible for them to separate monovalent salts and water from multivalent salts and low-molecular-weight organics[4]. NF benefits include low operating pressures, high rejection of divalent ions, particularly sulfates, removal of microorganisms, water turbidity, and a small amount of dissolved salts, and low energy consumption of 2.54 to 4.2 kWh/m [2]. However, its drawbacks include low rejection of boron and elevated levels of membrane fouling.

Forward Osmosis (FO) is a method for separating water from dissolved solutes that makes use of a semipermeable membrane and the natural energy of osmotic pressure to separate water from dissolved solutes. Osmotic pressure is used to transport water through the membrane. the feed solution flows on one side of the water membrane, while a draw solution with a higher total dissolved salinity (TDS) flows on the other side. The difference in TDS between the two sides creates osmotic pressure which induces water to flow from the feed solution through the membrane and into the draw solution while retaining all the contaminants in the feed stream.

Forward osmosis offers the advantage of producing concentrated brine and having less of an impact on the environment. However, the extraction solution recovery process requires a high amount of energy, up to 21 kWh/m3 [2].

The main advantages of the Reverse Osmosis (RO) technique include low space requirements, low energy consumption (2–6 kWh/m), and the RO can remove the dissolved solids (TDS) in water with an efficiency of about 95–99 %. While the RO's disadvantages include the membrane fouling, the durability, and the decline in water recovery with increasing scale.

The development of reverse osmosis began in the late 1950s when Reid et al. (1959) showed the use of compressed cellulose acetate membranes to slow the dispersion of salts while enabling the dispersion of water [5]. Later, as reverse osmosis developed, polyamide composite membranes were developed during the 1970s and 1980s [6]. When reverse osmosis was first tested on brackish water, it was later used for the treatment of seawater in the late 1970s, when commercial RO membranes were introduced for the first time. Reverse osmosis began to gain popularity in the middle of the 1980s and began to represent a difficult competition to thermal desalination [7]. Since its beginnings, reverse osmosis has made large achievements in terms of the development, resulting in higher product flux, improved salt rejection, reduced energy usage, and a decrease in total RO desalination costs.

For the development of RO processes, models that describe the operation of RO membranes are necessary. Reverse osmosis models can be described by a variety of mechanical and mathematical models. There have been several phenomenological and mechanistic theories set out to describe the transport of solutes and solvents through membranes. The research by Jinwen Wang et al.(1958) [8] showed that the membrane transport model may be classified into three more categories: the porous model, the irreversible thermodynamics model, and the non-porous model.

- The porous transport model is described in the literature by Sourirajan (1970) as a separation mechanism with holes on a membrane surface, where the pore size is twice the thickness of the water layer on that surface.
- The irreversible thermodynamic model described in Bitter (1991) in which the solute and solvent transport through the membrane is derived using irreversible thermodynamic concepts. Due to the concentration dependences of the phenomenological coefficients, the Kedem-Katchalsky and Spiegler-Kedem models in (1996) simplified the complicated design of this model. These models' limitations are that they are black-box-type models in which the transport processes are not fully explained.
- The non-porous model presented by Lonsdale et al. (1965) makes the assumption that the solute and solvent will dissolve and diffuse through the membrane along the concentration gradient. The homogeneous membrane model or the solution-diffusion model are other names for this one of the dense membranes that may be the most well-known.

Sundaramoorthy et al. [9] assumed a fixed value for each of the fluid viscosity, feed water density, permeate water density and the sea water diffusivity, this is due to the relatively tiny range of fluid temperature and concentration that he used in his experiments, which prevented any variation in these parameters. So, we developed that model using the necessary equations, to accommodate the relatively wide range of inlet operating conditions parameters. And S. Sundaramoorthy et al. [9] used chlorophenol salt in water as a solute in his experiments. But we used sodium chloride salt as a solute in our experiments, to represent seawater input in the desalination process. Where Artificial groundwater and seawater were prepared by adding salt to distilled water [10]. Additionally, we developed design equations that can be used with any type of water and a variety of salts as a solute in the solution.

Jamal et al. [11] created a model for a small-scale reverse osmosis system without applying concentration polarization, So, to account for the impact of concentration polarization on the membrane surface, we developed a mathematical model containing equations to predict this impact.

Al-Obaidi et al. [12] analyzed the performance of a multistage RO process under brackish water parameters with little variation in salinity.

Binns.[13] developed a mathematical model for a small-scale reverse osmosis system, validated it, and found it to be accurate, but he used only a narrow range of operation

Doi: 10.21608/ERJENG.2023.234375.1230

Journal of Engineering Research (ERJ)
Vol. 7 – No. 3, 2023
©Tanta University, Faculty of Engineering
ISSN: 2356-9441 https://erjeng.journals.ekb.eg/ e ISSN: 2735-4873

pressure and concentration, in order to account for the effects of them on water production.

Al-Obaidi et al. [14] improved a model-based simulation for a medium-scale brackish water desalination process. The model is validated on data from just brackish water using a restricted range of concentration utilizing data from a multistage RO system.

The existing literature has not yet employed a comprehensive and highly accurate reverse osmosis (RO) process model for the purpose of designing RO setups and optimizing their performance, especially when examining the behavior of spiral wound membranes under varying conditions of salinity, temperature, and pressure. This research study is concerned on addressing this gap. The primary objective of this study is to conduct a sensitivity analysis of the reverse osmosis process. This analysis delves into the performance metrics, including water recovery, salt removal efficiency, and the concentration of permeate water, under different intake conditions such as temperature, pressure, and feed salinity. Furthermore, to validate the proposed simulation model, experimental data from a pilot RO desalination unit, is utilized.

This study aims to assess the holistic impact of altering operating conditions within defined ranges and construct a mathematical model for SW (Seawater Reverse Osmosis) and BWRO (Brackish Water Reverse Osmosis) systems. Unlike the commercial software, which offered by membrane manufacturers, the present mathematical model provides greater flexibility in assessing process performance under various operating parameters and understanding the comprehensive consequences of changing these conditions within specified limits. Importantly, the present model is adaptable for use with any type of reverse osmosis membrane. To validate the accuracy and reliability of the model, experimental data obtained from the SWRO desalination plant are utilized to establish water parameters and permeability characteristics for the SWMAX4040 membrane element.

## II. MATHEMATICAL MODELING

Developing a comprehensive model for predicting and analyzing the performance of any industrial process is essential as a base for the design and optimization of this process. The present comprehensive model of the RO process is developed based on modifications and improvements on previous models in the literature, taking into account the effects of variation of parameters, e.g., density, which were neglected in the previous works. Also, the model parameters of the present model is estimated using a large number of experiments (250 experiment) conducted under a wider ranges of operating conditions, i.e., salt concentration, operating pressure and temperature, and flow rates.

### *1. Model development*

This model is established by applying material, mass, and energy balances on the general configuration depicted in Figure 1. The total material and mass balance are as follow:

Mass balances:

$$Q_f = Q_b + Q_p \tag{1}$$

Material balances:

$$Q_f C_f = Q_b C_b + Q_p C_p \tag{2}$$

where Q and C are the volumetric flow rate and the solute concentration respectively, and the subscripts f, b, and p stand for the feed, brine, and permeate sides, respectively.

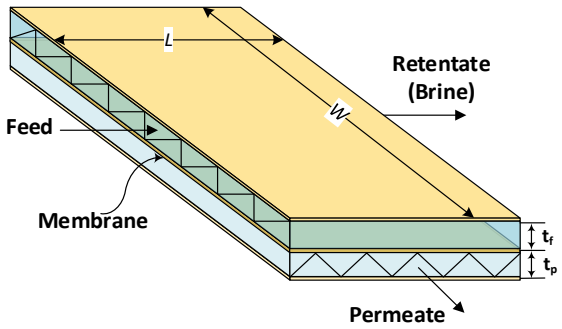


**Figure 1. Spiral wound RO membrane (unwound shape).**

The solution-diffusion model is believed to be valid for the RO process [15]. According to this model, the fluxes of the solvent, Jv, and the solute, Js, through the membrane are given as:

$$J_v = A_w \left(\Delta P - \Delta \pi\right) \tag{3}$$

$$J_s = B_s \left(C_b - C_p\right) \tag{4}$$

where $A_w$ and $B_s$ are the solvent and the solute transport parameters respectively, $\Delta P$ is the pressure difference across the membrane ( $\Delta P = P_b - P_p$ ), and $\Delta\pi$ is the difference in the osmotic pressure; from Vant hoff's relation [16]: $\Delta \pi = RT\left(C_b - C_P\right)$, $R$ is the gas constant and $T$ is the temperature.

By considering the impact of concentration polarization on the membrane's performance, the solute concentration at the membrane wall, CW, can be linked with both Cb and Cp as follows [17]:

$$C_W = C_P + \left(C_b - C_P\right)\exp\left(\frac{J_v}{K}\right) \tag{5}$$

where K is the diffusion mass transfer coefficient. Also, equations of $\Delta\pi$ and Js can be rewritten based on CW as:

$$\Delta \pi = RT\left(C_W - C_P\right) \tag{6}$$

Doi: 10.21608/ERJENG.2023.234375.1230

Journal of Engineering Research (ERJ)
Vol. 7 – No. 3, 2023
©Tanta University, Faculty of Engineering
ISSN: 2356-9441 https://erjeng.journals.ekb.eg/ e ISSN: 2735-4873

$$J_s = B_s\left(C_W - C_p\right) \tag{7}$$

Since the solvent flux is considerably higher than the solute flux, the following equation is applicable [18]:

$$J_s = J_v \cdot C_p \tag{8}$$

Substituting by Eqs. (6), (7), and (8) in Eq. (3), we obtain:

$$J_v = \frac{A_w \cdot \Delta P}{1+\left(\frac{A_w R}{B_s}\right)T \cdot C_p} \tag{9}$$

According to Eq. (9), the solvent flux Jv is a function of the permeate concentration Cp and the transmembrane pressure ΔP. An equation for the Cp can be obtained by combining Eqs. (5), (7) and (8) as:

$$C_p = \frac{C_b}{\left(1+\frac{\left(J_v/B_s\right)}{\exp\left(J_v/K\right)}\right)} \tag{10}$$

**Estimation the solvent and the solute transport parameters**

Every RO membrane is characterized by its Aw and Bs parameters values [19]. which both describes the membrane's permeability coefficient for pure water and salt, respectively.

In this section, The method for calculating the parameters Aw and Bs is developed graphically [9]. The following formula is used to compute the pressure drop (Pf−Pb) on the feed channel side:

$$P_{\mathrm{f}} - P_{\mathrm{b}} = \frac{bL}{\Phi \sinh \Phi}\left[\left(Q_{\mathrm{f}} + Q_{\mathrm{b}}\right)\left(\cosh \Phi - 1\right)\right] \tag{11}$$

where, the dimensionless parameter Φ [20] is given as:

$$\Phi = L\sqrt{\frac{WbA_{\mathrm{w}}}{\left(1+A_{\mathrm{w}}\left(\frac{R}{B_{\mathrm{s}}}\right)TC_{\mathrm{p}}\right)}} \tag{12}$$

the net pressure across the membrane at the feed inlet (Pf-Pp) is determined as follows:

$$P_{\mathrm{f}} - P_{\mathrm{P}} = \frac{bL}{\Phi \sinh \Phi}\left(Q_{\mathrm{f}} \cosh \Phi - Q_{\mathrm{b}}\right) \tag{13}$$

where b is the Friction coefficient for the feed channel. Also, a new dimensionless term β, we will use it to define the equation of parameter Φ, is defined as the ratio of the pressure drop (Pf−Pb) on the feed channel side to the net pressure across the membrane at the feed inlet (Pf-Pp). Substituting by Eqs. (11) and (13) we obtain:

$$\beta = \frac{\left(Q_{\mathrm{f}} + Q_{\mathrm{b}}\right)\left(\cosh \Phi - 1\right)}{Q_{\mathrm{f}} \cosh \Phi - Q_{\mathrm{b}}} \tag{14}$$

By rearranging the previous equation, we may calculate the parameter Φ as a function of the measured values of Qf, Qb, Pf, and Pb.

$$\Phi = \cosh^{-1}\left[\frac{\left(Q_{\mathrm{f}} + Q_{\mathrm{b}}\right) - \beta * Q_{\mathrm{b}}}{\left(Q_{\mathrm{f}} + Q_{\mathrm{b}}\right) - \beta * Q_{\mathrm{f}}}\right] \tag{15}$$

By rearranging the previous equation once more, and using the definition of Φ from Eq. (12), we obtain:

$$\frac{1}{\Phi^2} = \left(\frac{R}{L^2 WbB_{\mathrm{S}}}\right)TC_{\mathrm{P}} + \left(\frac{1}{L^2 WbA_{\mathrm{w}}}\right) \tag{16}$$

A straight-line fit is indicated by this equation on the plot of $1/\Phi^2$ vs T*$C_{\mathrm{p}}$, with slope: $S = \frac{R}{L^2 WbB_{\mathrm{S}}}$, and Intercept: $I = \frac{1}{L^2 WbA_{\mathrm{w}}}$ .by calculating the slope and intersection of a line we can Estimation $A_{\mathrm{w}}$ and $B_{\mathrm{s}}$ parameters values.

**Estimation of the membrane feed channel's friction coefficient (b).**

Similarly, From Eq.(11), A straight-line fit passing through the origin is indicated by this equation on the plot of $\left(P_{\mathrm{f}} - P_{\mathrm{b}}\right)$ vs $\frac{L}{\Phi \sinh \Phi}\left[\left(Q_f + Q_b\right)\left(\cosh \Phi - 1\right)\right]$ with slope=b.

## A. Model equations

mathematical modeling were developed by solving the model equations that were presented in this paper for the prediction of solvent flux (Jv), brine flow rate (Qb), pressure at the membrane output (Pb), permeate concentration and brine concentration Cp and Cb , respectively.

This section includes a set of important model equations needed to predict the flow rate, solvent flux, pressure, and solute concentration Q(x), Jv(x), Pb(x)and Cb(x), respectively. in the feed channel, at any position in membrane feed channel [20].

Doi: 10.21608/ERJENG.2023.234375.1230

Journal of Engineering Research (ERJ)
Vol. 7 – No. 3, 2023
©Tanta University, Faculty of Engineering
ISSN: 2356-9441 https://erjeng.journals.ekb.eg/ e ISSN: 2735-4873

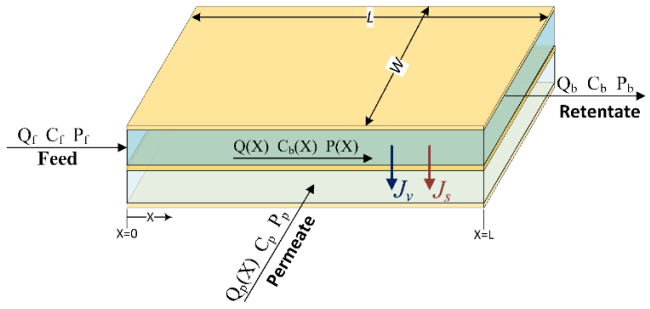


**Figure 2. Schematic representation of the spatial variations in a spiral wound reverse osmosis membrane module.**

$$Q(X)=\frac{Q_b \sinh\frac{\Phi X}{L}-Q_f \sinh\Phi\left(1-\frac{X}{L}\right)}{\sinh\Phi} \quad (17)$$

$$J_v(X)=\frac{\Phi}{A_w \sinh\Phi}\left[Q_f \cosh\Phi\left(1-\frac{X}{L}\right)-Q_b \cosh\frac{\Phi X}{L}\right] \quad \ldots(18)$$

$$P_b(X)=P_f-\frac{bL}{\Phi \sinh\Phi}\left[Q_f \cosh\Phi\left(1-\frac{X}{L}\right)-Q_b \cosh\frac{\Phi X}{L}\right] \quad \ldots(19)$$

$$C_b(X)=C_p+\frac{Q_f\left(C_f-C_p\right)}{Q(X)} \quad (20)$$

where, $\Phi$ is defined in Eq. (12), W is the width of the flat membrane that has been rolled up and placed inside the module and L is the module's length.

Determination of the solute flow Jv(x) at the membrane's inlet and outlet at x= 0 and x=L are:

$$J_V(in)=\frac{A_w * \Delta P_{in}}{1+\left(\frac{A_W R}{B_S}\right)TC_P} \quad (21)$$

$$J_V(out)=\frac{A_w * \Delta P_{out}}{1+\left(\frac{A_W R}{B_S}\right)TC_P} \quad (22)$$

where, the transmembrane pressure $\Delta P$ at x= 0 and x=L are $\Delta P_{in}=\left(P_f-P_p\right)$ and $\Delta P_{out}=\left(P_b-P_p\right)$ respectively.

The volume flow rate of retentate flow $Q_b$ and retentate pressure $P_b$ are calculated as follows:

$$Q_b=Q_f \cosh\Phi-\frac{\Phi \sinh\Phi}{bL}\Delta P_{in} \quad (23)$$

$$P_b=P_f-\frac{bL}{\Phi \sinh\Phi}\left[\left(Q_f+Q_b\right)\left(\cosh\Phi-1\right)\right] \quad (24)$$

From the material and mass balance Eq. (2), the concentration of brine is calculated as:

$$C_b=C_p+\frac{Q_f\left(C_f-C_p\right)}{Q_b} \quad (25)$$

Determination of the concentration of permeate $C_p$ at x= 0 and x=L are

$$C_p(in)=\frac{C_f}{\left[1+\frac{J_V(in)/B_S}{e^{J_v(in)}/K_{in}}\right]} \quad (26)$$

$$C_p(out)=\frac{C_b}{\left[1+\frac{J_V(out)/B_S}{e^{J_v(out)}/K_{out}}\right]} \quad (27)$$

where $k_{in}$ and $k_{out}$ are the mass transfer coefficients at the feed channel's inlet and outlet, respectively.

**Estimation of the coefficient of mass transfer (k)**

To determine the impact of different factors on mass transfer coefficient, the value of k was assumed to vary along the membrane feed channel with varying pressure, flow rate, and solute concentration conditions. As a result, the equations below were used to generate two values of mass transfer coefficients (K) [21], at the inlet and outlet of membrane feed channel.

At feed inlet (X= 0):

$$K_{in}=\frac{J_V(in)}{\ln\left[\frac{J_V(in)}{B_S}\left(\frac{C_p}{C_f-C_p}\right)\right]} \quad (28)$$

At feed outlet (X= L):

Doi: 10.21608/ERJENG.2023.234375.1230

Journal of Engineering Research (ERJ)
Vol. 7 – No. 3, 2023
©Tanta University, Faculty of Engineering
ISSN: 2356-9441 https://erjeng.journals.ekb.eg/ e ISSN: 2735-4873

$$K_{out} = \frac{J_V(out)}{\ln\left[\frac{J_V(out)}{B_S}\left(\frac{C_p}{C_b - C_p}\right)\right]} \quad (29)$$

The variation of *K* with regard to other factors showed that fluid velocity, solvent flow, solute concentration, and solute concentration had an impact on it. The mass transfer coefficient (k) also is calculated using the dimensionless number is defined as the Sherwood number $Sh = Kd_e/D_A$ . In this work, the Sherwood number is calculated using the following equation [20] since the membrane configuration used in this study is the same with that at [20].

$$Sh = 147.4 * \mathrm{Re}_p^{0.739} C_m^{0.135} \mathrm{Re}_f^{0.130} \quad ...(30)$$

where Permeate Reynolds number and Fluid Reynolds Number can be calculated as $\mathrm{Re}_p = (\rho_p d_e V_P)/\mu$ and $\mathrm{Re}_f = (\rho_f d_e V_f)/\mu$, respectively [22]. The fluid velocity at feed and permeate channel are defined as $V_f = Q_f/A_f$ and $V_P = J_V/A_P$, respectively.

Dimensionless solute concentration can be calculated as:

$$C_m = \frac{C_b}{\rho_m} \quad (31)$$

Feed channel and permeate channel cross-sectional areas are ( $A_f = t_f W$ ) and ( $A_p = t_p L$ ),respectively.

Another geometrical parameter required for the evaluation is the element's spacer-filled channel's hydraulic diameter. The following definition is usually used for flow channels with non-circular geometry [22]:

$$d_e = \frac{4 \times \textit{cross section of flow channel}}{\textit{wetted circumference}}.$$

The calculation for a flat channel ( $t_F \square W$ ) yields:

$$d_e = \frac{4Wt_f}{2(W + t_f)} = 2t_f \quad (32)$$

Here, de is a rectangular feed channel's equivalent diameter with a thickness of tf, can be calculated as:

$$d_e = 2t_f \quad (33)$$

Concentration in Eq. 31 must be multiplied by $C_v$ to translate from ppm to kmole/m$^3$, where $C_v$ take the value of 0.0171108.

The feed seawater and permeate water density can be calculated as [23]:

$$\rho_f = 498.4m + \sqrt{\left[248400m^2 + 752.4 * 10^{-3} * mC_f * C_v\right]} \quad ...(34)$$

$$\rho_P = 498.4m + \sqrt{\left[248400m^2 + 752.4 * 10^{-3} * mC_P * C_v\right]} \quad (35)$$

Where

$$m = 1.0069 - 2.757 * 10^{-4} \times T/273.15$$

Fluid viscosity can be calculated as follow [23]:

$$\mu = 1.234 * 10^{-6} * \exp\left(0.00212 * 10^{-3} * C_b * C_v + \frac{1965}{T}\right) \quad (36)$$

The diffusivity of seawater in m2 /s is given as in [23]as follows;

$$D = 6.725 * 10^{-6} * \exp\left(0.1546 * 10^{-6} C_b * C_v - \frac{2513}{T}\right) \quad (37)$$

To predict RO performance and optimize energy usage as well as permeate quality, we used the concentration polarization theory modified version of the solution-diffusion model.

The model derivation was based on the following assumptions: an RO membrane module is made up of flat channels with spacers. The solute concentration has no effect on the diffusion coefficient.

- Along a RO element, the brine concentration varies linearly.
- The concentration polarization effect may be calculated using the thin film theory.
- The permeate side pressure drop is neglected.
- Mass transfer coefficient is constant for a given fluid condition.
- While the feed flow rate varies depending on the recovery, the permeate flow rate remains constant.
- The high-pressure feed pump is responsible for most of the energy used in the RO process.

## III. EXPERIMENTAL SET-UP

The RO experimental test rig was set up as seen in Figure 4 on the roof of Faculty of Engineering, Tanta University. All the experiments were conducted during the summer of 2022. The experiments were carried out in an effort to improve the performance of the RO unit and used to validate the results of this simulation model. This section is divided into two main parts, as shown in Figure 3. The first part describes the

Doi: 10.21608/ERJENG.2023.234375.1230

Journal of Engineering Research (ERJ)
Vol. 7 – No. 3, 2023
©Tanta University, Faculty of Engineering
ISSN: 2356-9441 https://erjeng.journals.ekb.eg/ e ISSN: 2735-4873

experimental test-rig which contains the experimental apparatus. The second part is devoted to provide a brief description of the employed measuring techniques and instrumentation. The design and construction of the experimental setup is also presented.

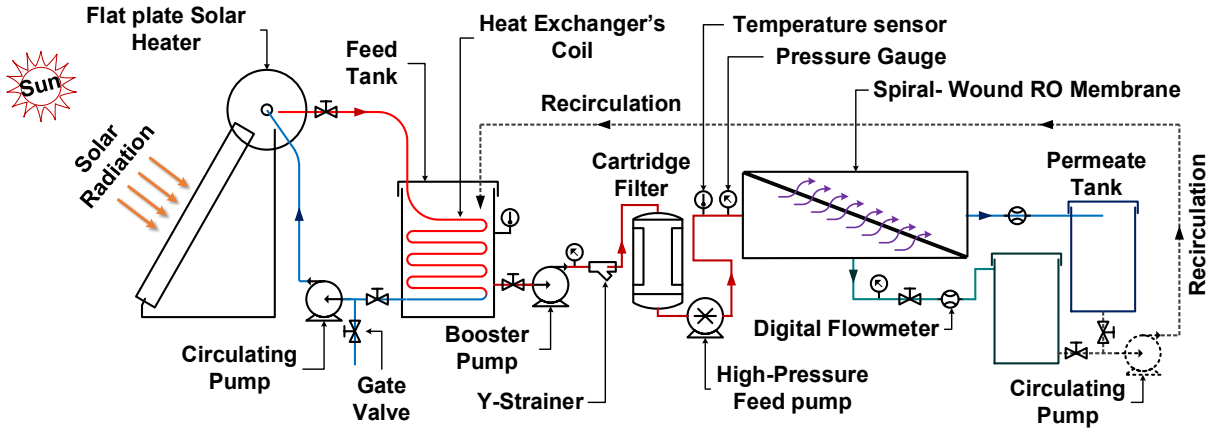


Figure 3. Present work schematic diagram.

**A) Synthetic Groundwater and Seawater**

Due to the requirement of brackish groundwater and Conventional seawater wells in large quantities, artificial groundwater and seawater were prepared. The artificial groundwater and seawater were prepared by adding salt in distilled water [18]. A tank with capacity 1000 L of distilled water was used to make the artificial groundwater and seawater sample.

**B) Experimental Setup**

The unit consists of two loops. The first loop is solar water collector loop. Water is heated in the solar water heater (SWH), then hot water from solar collector is transferred to heat exchanger in feed water tank. In feed water tank, salt concentration is set, and feed water temperature is controlled at specified temperature using the heat exchanger. The second loop is the desalination process in which feed water is circulated to pretreatment stage by feed pump located between feed water tank and cartridge filter. The feed water passes through the y-strainer and the cartridge filter to remove any suspended particles in the water before compressing the water to the membrane module by the high-pressure pump. A closed loop is created by the brine and permeate water that exits from the membrane then are collected in the brine and permeate tanks is sent back to the feed water tank after the experiment by circulate pump (1).

**C) Solar Water Collector**

Fresh water was heated by a pressurized solar water heater type of flat plate collector, which model number is (P-G0.8-TA-LT-1.88) as shown in Figure. And connected with pressure stainless steel storage tank capacity is 300 liters, The storage tank type is (PJF1-300-420/500-D-09).

Two solar water collectors were used, and they were connected in series. The dimensions of the flat plate collectors heat-absorbing area for each of them are 2m x 1m.

**D) RO Desalination Plant**

The RO unit with a capacity of 6.62 $m^3$ of fresh water per day was used. The unit consists of two stages: the first stage is a pretreatment for the feed water, in which the feed water initially passes through bag and micron filters, which is then pumped by high-pressure pumps to the RO membrane. In this stage the feed pump (1.7 hp centrifugal pump) pressurized the feedwater from the feed tank to the Y- strainer which its purpose is to remove unwanted particles from liquid using a straining element typically made of wire mesh. Then the water pass through the cartridge filter with a porosity of 5 µm is a piece of tubular filtration equipment that can be used for removing unwanted particles, pollutants, and chemicals from liquids. Cartridge filters can also remove submicron particulates. The second stage is the RO desalination unit consists of a high-pressure pump type of Reciprocating Triplex Plunger Pumps model (NLT3020IR) from HAWK International company, and a SWC5-LD-4040 membrane from Hydranautics – A Nitto Group Company. The membrane's characteristics and limitations of Operating parameters are summarized in Table 1.

The process is measured by pressure gauges in different parts in the system. we use two types (Bourdon Tube Pressure Gauge), one of them which ranges up to 25 bar, and another up to 100 bar.

We used Digital Flow Meter magnetic-inductive flow meter with model number (SM6000) to find out flow rate of product water or brine flow rates also we can find out the feed flow rate by using the valves control and changing the pass of water

Doi: 10.21608/ERJENG.2023.234375.1230

Journal of Engineering Research (ERJ)
Vol. 7 – No. 3, 2023
©Tanta University, Faculty of Engineering
ISSN: 2356-9441 https://erjeng.journals.ekb.eg/ e ISSN: 2735-4873

inter to the flow meter. And we used Variable Area Flowmeter or Rotameter in the line of the permeate and the brine water as indicators. For the salt concentration measurement, we used (ProQuatro) Multiparameter Meter model number (SKU6050000) which can measure conductivity, salinity, total dissolved solids (TDS), pH, and temperature. For the water temperature measurement, we used (ProQuatro Multiparameter) mainly to measure, and used Digital Thermometer Sensor LCD Display-Waterproof Probe as indicators. The specifications and accuracy of measurements devices are shown in Table 2.

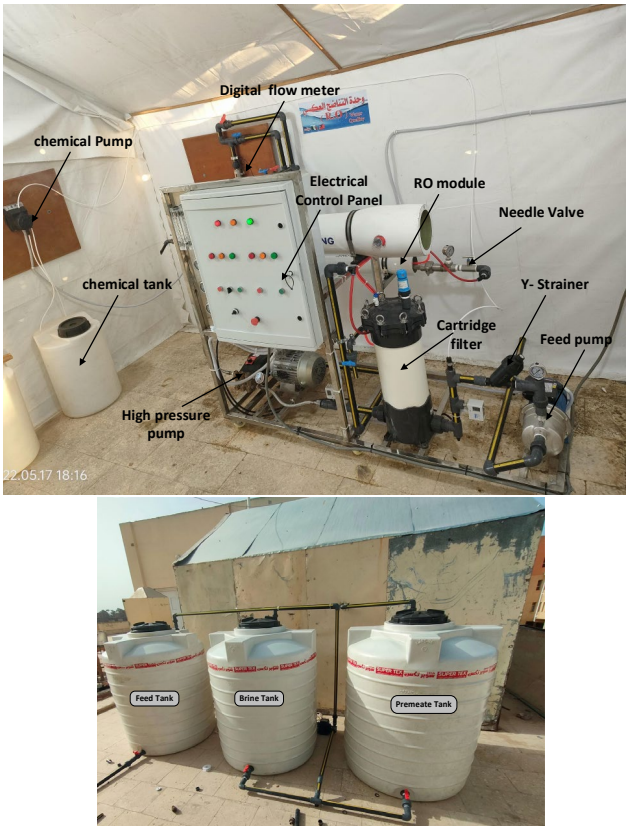





**Figure 4. Photos of the RO unit and the experimental setup used in this study.**

**Table 1. General Product (Membrane) Description**

| | |
|---|---|
| Configuration | Low Fouling Spiral Wound Membrane |
| Polymer | Composite Polyamide |
| Membrane Active Area | 80 $ft^2$ (7.43 $m^2$) |
| Feed Spacer | 34 mil (0.864 mm) |
| RO unit with a capacity | 6.62 ($m^3$/day) |
| Operating parameters of the RO membrane | |
| Maximum Applied Pressure: | 1200 psi (82.7bar) |
| Maximum Operating Temperature | 113 ˚F (45 ˚C) |
| Maximum Feed Flow | 16 gpm (3.6 $m^3$/h) (60 l/min) |
| Maximum Pressure Drop for Each Element | 15 psi (0.10 MPa) (1 bar) |

**Table 2. specifications of measurements devices**

| Measurements devices | Parameter | Range | Accuracy |
|---|---|---|---|
| The ProQuatro Multiparameter meter's | Temperature (°C) | 0 to 40°C | ±0.35°C |
| | Total Dissolved Solids (TDS), (ppm) | 0 to 128000 PPM | ±1.0% of reading |
| Digital Thermometer Sensor | Temperature (°C) | -50 to 110°C | ± 0.1 °C |
| Digital flow meter | Flowrate (l/min) | 0.1- 25 l/min | ± 0.145 l/min |
| Bourdon Tube Pressure Gauge | Pressure, (bar) | up to 25 bar | ±0.25 bar |
| | | up to 100 bar | ±1 bar |

**Test procedures and data collection**

- We first prepare and fill the solar water collector at least a day before doing the experiments, in order to ensure that there is hot water available in the heat exchanger loop between the solar collector and the feed tank.
- To make sure there is no salt scaling or fouling on the RO membrane, we flush or clean it by turning on the feed pump in the system with tap water.
- Turn on first valve to fill feed water tank with water from tap water line and dissolve salt in the water to set salt concentration needed of feed water, then solar water collector loop operates by turn on Circulation pump (2) to transfer the energy of the hot water from the solar water collector to heat exchanger in feed tank to set the temperature of feed water at specified temperature.
- In the beginning, we used a device (ProQuatro Multi parameter), in order to check all the feed water's temperature and salinity in the feed tank needed to conduct the experiment.
- Turn on the feed water pump to start the operation of the pretreatment stage, and to ensure that there is no air in the lines or in the membrane module.
- Turn on the high-pressure pump, and then manually regulate the frequency of the electrical power received by the pump by using the variable frequency drive to control the high-pressure pump speed. This will allow a fixed amount of feed water to flow to the RO membrane module.
- After the pretreatment stage, we recheck the temperature and salinity of the feed water by taking a sample of the water through a tap after the cartridge filter housing.
- Then, using the needle valve that has been fitted at the membrane's end at the brine outlet, we manually regulate the feeding pressure.
- Let the system run for a few minutes to reach a steady state, and run measurement devices and check them.
- Using a digital flow meter, we record both the permeate and brine water flow rates.
- We record the brine and permeate water temperatures and concentrations of salt at the output of the membrane from taps in storage tanks.

Doi: 10.21608/ERJENG.2023.234375.1230

Journal of Engineering Research (ERJ)
Vol. 7 – No. 3, 2023
©Tanta University, Faculty of Engineering
ISSN: 2356-9441 https://erjeng.journals.ekb.eg/ e ISSN: 2735-4873

- After using the RO unit and finishing our test of the experiment, it is highly possible that impurities or salt scaling may clog inside the RO housing and on the RO membrane. So, it is highly recommended to clean the housing and the membrane after using a RO system, by flushing them with tap water.

**Mathematical Modeling Procedure**

Figure 5 shown the flow chart of Mathematical Modeling Procedure, the MATLAB/ code script software version R2016a was used to build a mathematical model to analyze the design and examine the performance of any reverse osmosis system. This model is designed based on theory of solution diffusion model and the results obtained from the experimental work. Comparing the properties of flow and mass transfer coefficient to the real data obtained from the experimental work. since the feed temperature, feed concentration, feed pressure, and flow rate were all affected by the designed model.

**Sensitivity analysis of RO membrane process**

This section does a sensitivity analysis of the spiral wound RO membrane process. The purpose of this simulation is to ascertain the overall effect of varying the operating conditions within certain parameters. In this regard, it was planned for the simulation of this study to evaluate the responses to change in one input parameter at a time while other parameters remaining fixed. The selected seawater inlet parameters that will be used in the RO membrane process is changed in range for feed concentration from 10000 to 30000 ppm, and feed pressure from 12 to 40 bar.

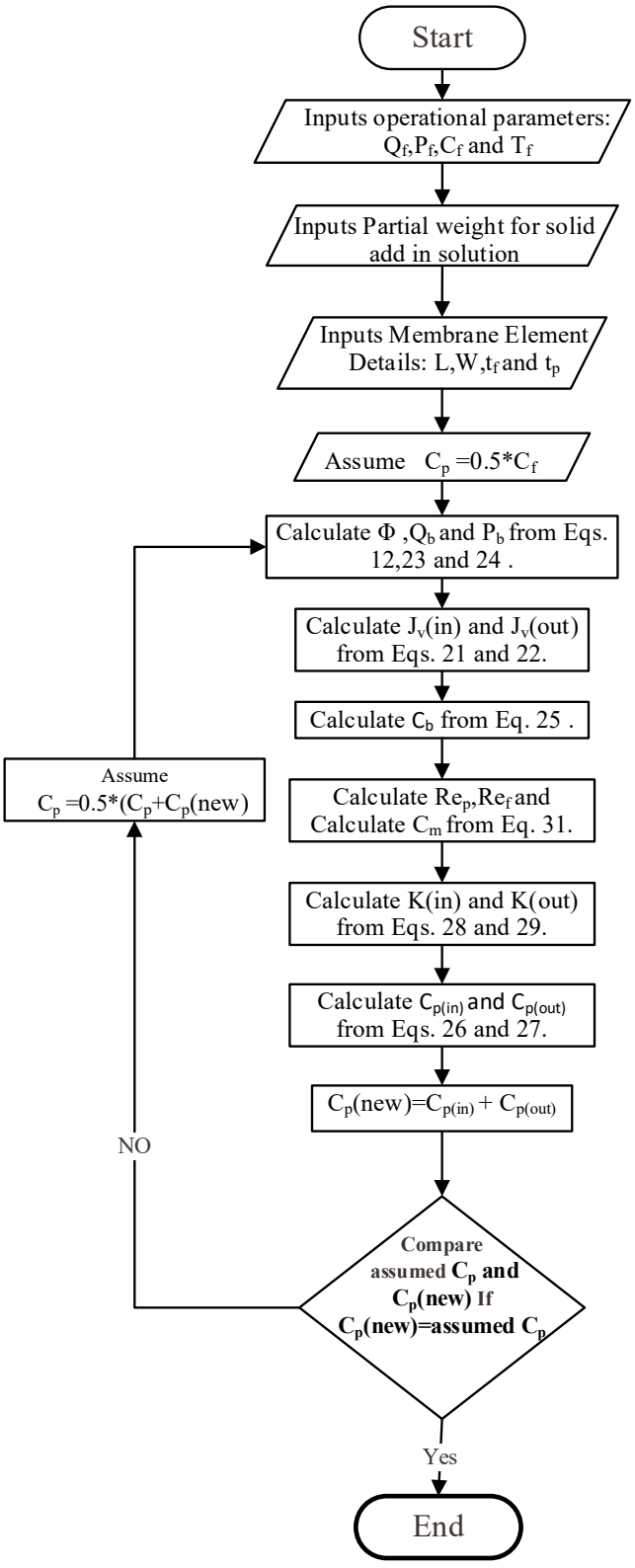


**Figure 5. Flow chart of Mathematical Modeling Procedure.**

Doi: 10.21608/ERJENG.2023.234375.1230

Journal of Engineering Research (ERJ)
Vol. 7 – No. 3, 2023
©Tanta University, Faculty of Engineering
ISSN: 2356-9441 https://erjeng.journals.ekb.eg/ e ISSN: 2735-4873

**Uncertainty analysis**

Uncertainty analysis is a useful tool to determine the calculated and measured uncertainties. The measured parameters uncertainty consists of systematic errors, including data acquisition, calibration, and equipment accuracy, and random errors. The standard deviation method was applied to determine the total uncertainty according to Holman [23].

Let result is a given function of the independent variables $X_1$, $X_2$, …., $X_n$

$R=R(X_1, X_2, X_3 \ldots X_n)$

Let $W_R$ be the uncertainty in the result and $W_1$, $W_2$, $W_3$,…, $W_n$ be the uncertainties in the independent variables X1, X2, X3,……., Xn respectively.

$$W_R = \left[ (W_1 \partial R/\partial X_1)^2 + (W_2 \partial R/\partial X_2)^2 + (W_3 \partial R/\partial X_3)^2 + \ldots + (W_n \partial R/\partial X_n)^2 \right]^{0.5} \quad \ldots(39)$$

The relative error can be calculated as follows.

$E_R = W_R/R\%$

The calculated errors are:

- For salt rejection (SR) are $W_R = \pm 0.0004\%$, and $E_R = \pm 0.04\%$.
- For Brine flow rate ($Q_b$) are $W_R = \pm 0.145\ \%$, and $E_R = \pm 0.145\ \%$.

## IV. RESULTS AND DISCUSSION

In This section, the theoretical results of the MATLAB program's mathematical modeling are discussed. The effect of various operational and geometrical parameters on the performance of membrane modules is evaluated as seen below:

**A. Calculation of the Salt and Water Transport Coefficients ($A_w$ and $B_s$) and the Pressure Coefficient (b)**

Every RO membrane is characterized by its Membrane A and Membrane B values [9]. Membrane A value is the membrane's permeability coefficient for pure water. Membrane B value is the salt permeability coefficient of the membrane.

In this section the values of the salt and water transport coefficients ($A_W$ and $B_S$) may be calculated by graphing ( $1/\phi^2$ ) vs (T*Cp), as was indicated in chapter 2 (mathematical modelling).

By using the equation of the pressure drop across the membrane as shown below.

$$P_{in} - p_{out} = \frac{bL}{\varnothing \sinh \varnothing}\left[ (F_{in} + F_{out})(\cosh \varnothing - 1) \right] \quad \ldots(40)$$

From the drawing of $P_{in} - p_{out}$ vs $\frac{L}{\varnothing \sinh \varnothing}\left[ (F_{in} + F_{out})(\cosh \varnothing - 1) \right]$ in Figure 4 is a straight line passing through the origin with a slope of S2 equal to b.

S2 = b

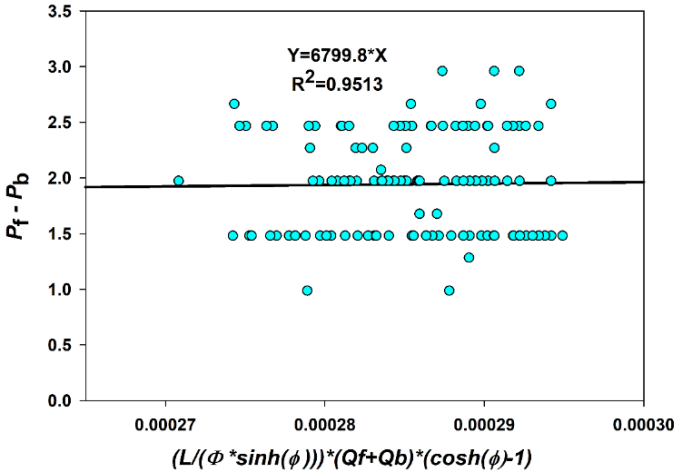


**Figure 4. plot of $P_{in} - p_{out}$ vs $\frac{L}{\varnothing \sinh \varnothing}\left[ (F_{in} + F_{out})(\cosh \varnothing - 1) \right]$ from experimental data with linear fitting**

Similarly, by using the definition of Φ and rearranging the terms in this equation, we obtain:

$$\frac{1}{\varnothing^2} = \left( \frac{\gamma}{L^2 W b B_S} \right) TC_P + \left( \frac{1}{L^2 W b A_W} \right) \quad \ldots(41)$$

This equation represents a straight line fit on the plot of $1/\phi^2$ vs $T*C_p$ (Figure 5) with slope S and Intercept I.

Where:

$$S = \frac{\gamma}{L^2 W b B_S} \quad \ldots(42)$$

$$I = \frac{1}{L^2 W b A_W} \quad \ldots(43)$$

Doi: 10.21608/ERJENG.2023.234375.1230

Journal of Engineering Research (ERJ)
Vol. 7 – No. 3, 2023
©Tanta University, Faculty of Engineering
ISSN: 2356-9441 https://erjeng.journals.ekb.eg/ e ISSN: 2735-4873

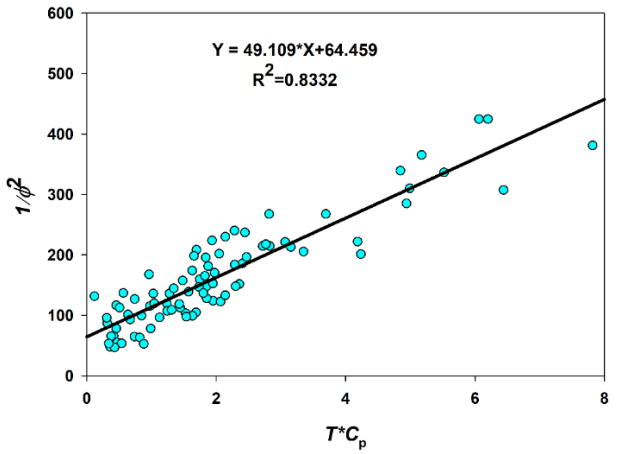


**Figure 5. plot of $1/\phi^2$ vs T*$C_p$ from experimental data with linear fitting.**

The estimated values of $b$, $A_w$, and $B_s$ are given in Table 3 .

**Table 3. Value of model parameters $A_W$, $B_S$, and $b$**

| Parameters | Value |
|---|---|
| b ( $atm.s / m^4$ ) | 6799.8 |
| $A_W$ ( $m / atm.s$ ) | $3.11349*10^{-7}$ |
| $B_S$ ( $m / s$ ) | $3.35107*10^{-8}$ |

### *A. Model Validation*

This part uses the model validation against a set of experimental data obtained from the RO system at the college of engineering at Tanta University in Egypt to measure the validity of the model described above. This is specifically carried out by comparing the collected data with the prediction made by the model. The model validation is shown in Figure 6 below with an average accuracy of above 98%. The model equations were solved using the MATLAB (MATLAB/ code script software version R2016a) model builder. The predictions of our model show very good agreement with experimental work.

The model predictions for brine flow $F_o$, brine concentration $C_o$, permeate concentration $C_p$, water recovery Re, and salt rejection coefficient SR were calculated using the mathematical modeling method for each reading in the experimental calculation. As shown in Table 4 The model can predict the values of water recovery Re with an average error 4.0578% of the readings, and rejection coefficient SR with an average error 0.2755 % of the readings, it is clear from comparing the model predictions with the experimental observations. The predictions of our model show very good agreement with those of mathematical modeling methods for the large variety of operation parameters conditions that were studied and analyzed.

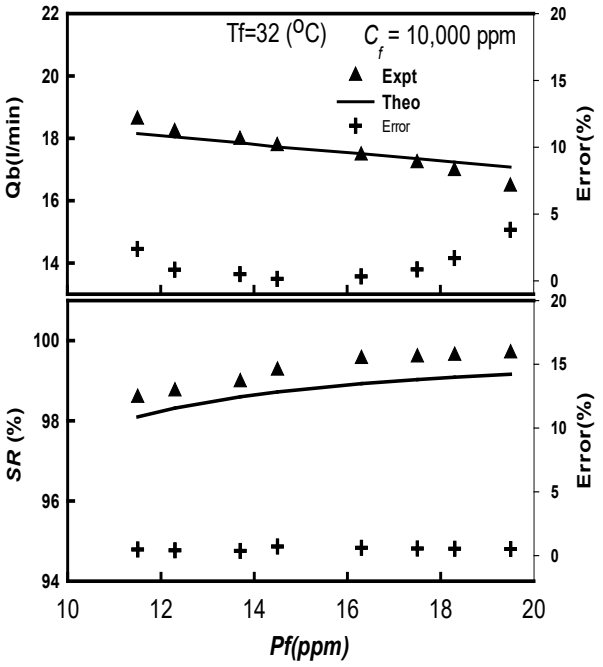


(A)

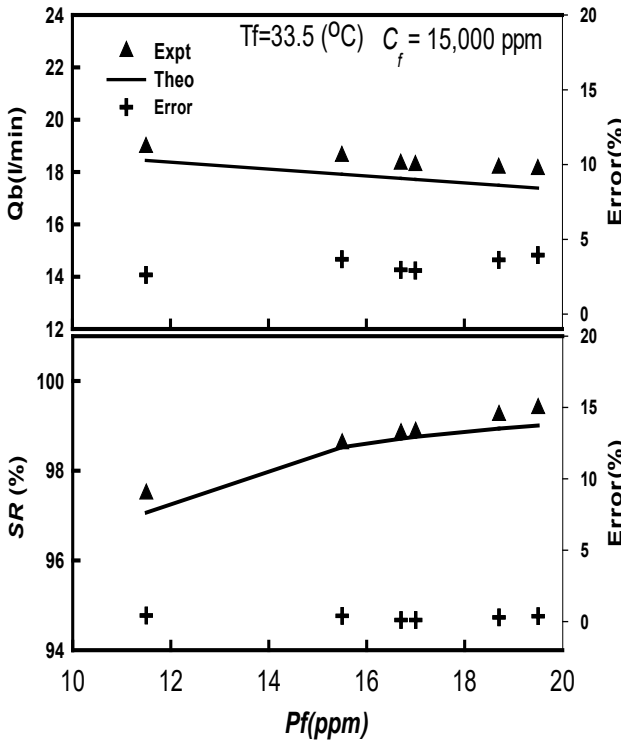


(B)

Doi: 10.21608/ERJENG.2023.234375.1230

Journal of Engineering Research (ERJ)
Vol. 7 – No. 3, 2023
©Tanta University, Faculty of Engineering
ISSN: 2356-9441 https://erjeng.journals.ekb.eg/ e ISSN: 2735-4873

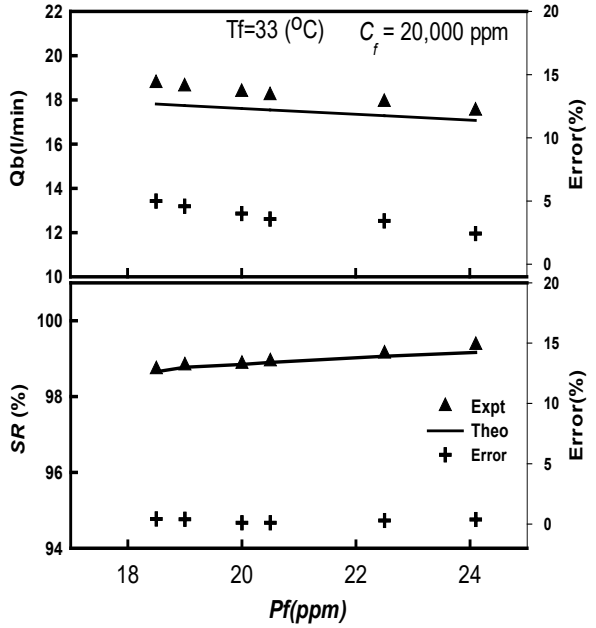


(C)

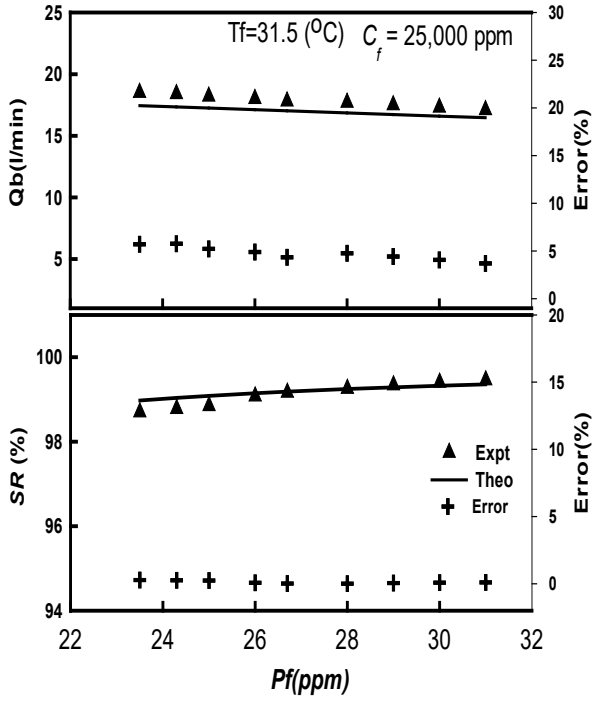


(D)

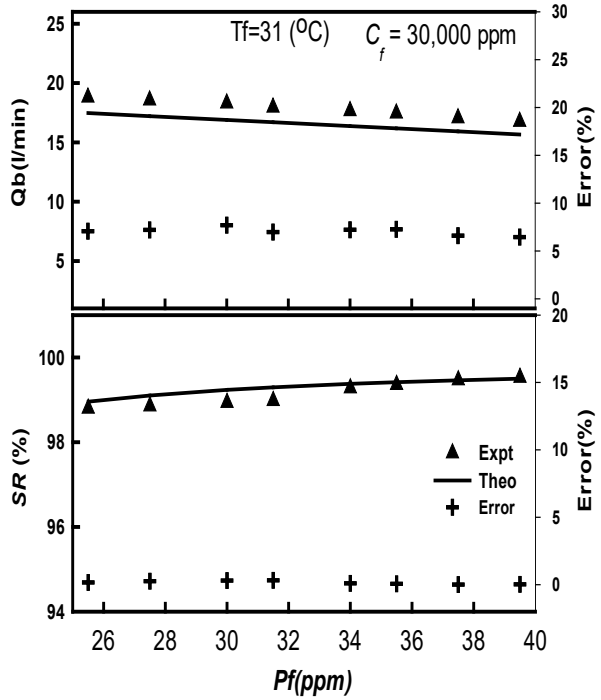


(E)

**Figure 6. A, B, C, D and E. display the Model validation with experimental data. brine flow rates, and salt rejection ratio of the theoretical model were compared with experimental results at different feed pressure, and at fixed feed flow rate Qf=18.95 L/min., when feed water salinity is (A) Cf=10000 ppm, (B) Cf=15000 ppm, (C) Cf=20000 ppm, (D) Cf=25000 ppm, and (E) Cf=30000 ppm.**

**Table 4. Error percentages between experimental and theoretical data on brine flow rate (Qb), and salt rejection (SR) in the spiral wound RO module at a feed flow rate of Qf= 18.95 (L/min.)**

| $C_f$, (ppm) | $P_f$ (bar) change | | $T_f$, (°C) | $Q_b$ (Error)% | | | SR (Error)% | | |
|---|---|---|---|---|---|---|---|---|---|
| | From | TO | | MIN | MAX | MEAN | MIN | MAX | MEAN |
| 10000 | 12 | 20 | 32 | 0.15 | 3.82 | 1.33 | 0.37 | 0.72 | 0.53 |
| 15000 | 12 | 20 | 33.5 | 2.62 | 3.95 | 3.29 | 0.11 | 0.42 | 0.29 |
| 20000 | 18 | 24 | 33 | 2.43 | 4.99 | 3.84 | 0.11 | 0.42 | 0.29 |
| 25000 | 24 | 31 | 31.5 | 3.71 | 5.77 | 4.77 | 0.01 | 0.28 | 0.12 |
| 30000 | 25 | 40 | 31 | 6.46 | 7.70 | 7.07 | 0.01 | 0.32 | 0.15 |

Regarding the effect of feed water pressure, Figure 6 shows a decrease in brine flow rate that means an increase in water productivity, and the SR through the membranes increase at a slower pace with an increase in pressure at fixed feed flowrate, salinity, and temperature. It is found that increasing feed pressure has a significant impact on water productivity by an average increase of 1.108 %, however, as input pressure was increased by less than 1bar, and the solute rejection increased

Doi: 10.21608/ERJENG.2023.234375.1230

Journal of Engineering Research (ERJ)
Vol. 7 – No. 3, 2023
©Tanta University, Faculty of Engineering
ISSN: 2356-9441 https://erjeng.journals.ekb.eg/ e ISSN: 2735-4873

0.242 %. This behavior is explained by the fact that raising the feed pressure would lead in an increased water flux, which would raise the permeate flowrate and improve water productivity.

Regarding the effect of feed water concentration, water productivity and salt rejection SR decrease as feed water concentration increases. This may be explained by an overall decrease in the Net driving pressure caused by the growing osmotic pressure differential across the membrane, and the RO membrane process is essentially a water filtration method, any increase in feed salinity will increase the bulk salinity and the discharged salinity, causing the retentate salinity to increase without a doubt.

Regarding the effect of feed water temperature, with the increase in feed water temperature, we found an improvement in water productivity and found a decrease in the brine flow rate. This is explained by the fact that increasing the feed temperature caused the viscosity and density properties to decrease. As a result, raising the provided temperature is projected to increase the diffusion of water through the membrane.

## V. CONCLUSION

This study develops an accurate mathematical model for describing the performance of RO membrane under different operating conditions based on a seawater spiral-wound membrane, and the model developed an algorithm developed on MATLAB software using the solution-diffusion and mass transfer theories, in order to comprehend the impacts of pressure, salt concentration, temperature, and flow rate of feed water on the process performance as shown by the rates of permeation and salt rejection. As a result, this strategy offers a simple method to create the predictive model. In comparison to the more complex numerical type models, which require solving much larger numbers of equations and requiring more computational effort. An experimental system has been set up for measuring the flow rate, and concentration of brine and permeate at different applied pressures, temperatures, flow rate, and feed concentration. The model validation analysis showed that the mathematical modeling prediction results were in good agreement with the experimental data with an average accuracy of above 98%, with an average inaccuracy of 4.0578% for predicting the values of water productivity and 0.2755% for predicting the salt rejection coefficient.

Regarding the future research work, here are some potential research directions in RO, including (1) Investigate novel materials and structures to improve membrane effectiveness and longevity, (2) Explore methods to reduce fouling and scaling issues in RO systems, (3) Consider solar or wind power for sustainable RO processes, particularly in energy-constrained regions, (4) And finally, use machine learning and AI for real-time RO system control, enhancing performance and energy efficiency.

### Nomenclature

| | |
|---|---|
| $A_f$ | Feed channel area, ($m^2$) |
| $A_m$ | Membrane surface area, ($m^2$) |
| $A_p$ | Permeate channel area, ($m^2$) |
| $A_w$ | Solvent transport coefficient, (m/atm·s) |
| $b$ | The Friction coefficient for the feed channel, (atm·s/$m^4$) |
| $B_s$ | Solute transport coefficient, (m/s) |
| $C_b$ | The retentate(brine) concentration, (kmol/$m^3$) |
| $C_{b(x)}$ | The feed concentration at X, (kmol/$m^3$) |
| $C_f$ | The feed concentration, (kmol/$m^3$) |
| $C_m$ | Dimensionless solute concentration in Eq. (30) |
| $C_p$ | The permeate concentration, (kmol/$m^3$) |
| $C_{p(in)}$ | The permeate concentration Cp at x= 0, (kmol/$m^3$) |
| $C_{p(new)}$ | Assumed value of Cp in the iterative calculation steps, (kmol/$m^3$) |
| $C_{p(out)}$ | The permeate concentration Cp at x= L, (kmol/$m^3$) |
| $C_w$ | The solute concentration at the membrane wall, (kmol/$m^3$) |
| $D$ | Diffusivity of seawater, ($m^2$/s) |
| $de$ | Feed channel Equivalent diameter, (m) |
| I | Intercept |
| $J_s$ | Solute flux, (kmol of solute/$m^2$.s) |
| $J_v$ | Solvent flux, (m/s) |
| $J_{v(in)}$ | Solvent flux Jv(x) at x= 0, (m/s) |
| $J_{v(out)}$ | Solvent flux Jv(x) at x=L, (m/s) |
| $J_{v(x)}$ | Solvent flux at x, (m/s) |
| $K$ | The diffusion mass transfer coefficient, (m/s) |
| $k_{in}$ | Mass transfer coefficient at the inlet, (m/s) |
| $k_{out}$ | Mass transfer coefficient at the outlet, (m/s) |
| $L$ | RO module length, (m) |
| $m$ | Empirical constant defined by Eq. (34 and 35) |
| $P_b$ | Retentate (brine) pressure, (atm) |
| $P_{b(x)}$ | Water pressure at x, (atm) |
| $P_f$ | Membrane Feed pressure, (atm) |
| $P_p$ | Permeate pressure, (atm) |

Doi: 10.21608/ERJENG.2023.234375.1230

Journal of Engineering Research (ERJ)
Vol. 7 – No. 3, 2023
©Tanta University, Faculty of Engineering
ISSN: 2356-9441 https://erjeng.journals.ekb.eg/ e ISSN: 2735-4873

| | |
|---|---|
| $Q_{(x)}$ | The flow rate, ($m^3$/sec) |
| $Q_b$ | Brine flow rate, ($m^3$/sec) |
| $Q_f$ | Membrane Feed flow rate, ($m^3$/sec) |
| $Q_p$ | Permeate flow rate, ($m^3$/sec) |
| $R$ | The gas constant |
| $Re_f$ | Fluid Reynolds number, (–) |
| $Re_p$ | Permeate Reynolds number, (–) |
| s | Slope |
| $Sc$ | Schmidt number, (–) |
| $Sh$ | Sherwood number, (–) |
| $T$ | Water Temperature, (K) |
| $t_f$ | Feed spacer thickness, (mm) |
| $t_P$ | Permeate channel thickness, (mm) |
| $V_f$ | The feed velocity feed and permeate, (m/s) |
| $V_p$ | The permeate fluid velocity, (m/s) |
| $W$ | RO module width, (m) |
| $x$ | Axial position in feed channel, (m) |

**Greek symbols**

| | |
|---|---|
| $\beta$ | A dimensionless parameter, defined in Eq. (14 and 15) |
| $\gamma$ | The gas law constant, (0.08206 L atm /mol K) |
| $\Delta$ | Difference across the membrane |
| $\Delta p$ | The transmembrane pressure, (atm) |
| $\Delta P_{in}$ | The transmembrane pressures at x= 0, (atm) |
| $\Delta P_{out}$ | The transmembrane pressures at x= L, (atm) |
| $\mu$ | Viscosity, (kg/m.s) |
| $\pi$ | Osmotic pressure, (atm) |
| $\rho_f$ | Feed water density, ($kg/m^3$) |
| $\rho_m$ | Molal density of water, (55.56 $kmol/m^3$) |
| $\rho_p$ | Permeate density, ($kg/m^3$) |
| $\Phi$ | Dimensionless term, (–) |
| $\Delta\pi$ | The osmotic pressure difference, (atm) |

**Funding**: The authors should mention if this research has received any type of funding.

**Conflict of Interest**: The authors declare that there is no conflict of interests regarding the publication of this paper.

## REFERENCES

[1] World Health Organization (WHO), "Hardness in drinking-water: background document for development of WHO guidelines for drinking-water quality," 2010. https://apps.who.int/iris/bitstream/handle/10665/70168/WHO_HSE_WSH_10.01_10_Rev1_eng.pdf
[2] J. J. Feria-Díaz, F. Correa-Mahecha, M. C. López-Méndez, J. P. Rodríguez-Miranda, and J. Barrera-Rojas, "Recent desalination technologies by hybridization and integration with reverse osmosis: A review," Water (Switzerland), vol. 13, no. 10, pp. 1–40, 2021, doi: 10.3390/w13101369.
[3] M. Bin Abid, R. A. Wahab, M. A. Salam, L. Gzara, and I. A. Moujdin, "Desalination technologies, membrane distillation, and electrospinning, an overview," Heliyon, vol. 9, no. 2, p. e12810, Feb. 2023, doi: 10.1016/J.HELIYON.2023.E12810.
[4] N. N. R. Ahmad, A. W. Mohammad, E. Mahmoudi, W. L. Ang, C. P. Leo, and Y. H. Teow, "An Overview of the Modification Strategies in Developing Antifouling Nanofiltration Membranes," Membranes, vol. 12, no. 12. 2022. doi: 10.3390/membranes12121276.
[5] C. E. Reid and E. J. Breton, "Water and ion flow across cellulosic membranes," J. Appl. Polym. Sci., vol. 1, no. 2, pp. 133–143, 1959, doi: 10.1002/app.1959.070010202.
[6] O. K. Buros, R. B. Cox, I. Nusbaum, A. M. El-Nashar, and R. Bakish, "The U.S.A.I.D. Desalination Manual," no. August. p. 469, 1981.
[7] L. F. Greenlee, D. F. Lawler, B. D. Freeman, B. Marrot, and P. Moulin, "Reverse osmosis desalination: Water sources, technology, and today's challenges," Water Res., vol. 43, no. 9, pp. 2317–2348, May 2009, doi: 10.1016/J.WATRES.2009.03.010.
[8] J. Wang et al., "A critical review of transport through osmotic membranes," J. Memb. Sci., vol. 454, pp. 516–537, Mar. 2014, doi: 10.1016/J.MEMSCI.2013.12.034.
[9] S. Sundaramoorthy, G. Srinivasan, and D. V. R. Murthy, "Reprint of: 'An analytical model for spiral wound reverse osmosis membrane modules: Part II — Experimental validation,'" Desalination, vol. 280, no. 1–3, pp. 432–439, Oct. 2011, doi: 10.1016/J.DESAL.2011.08.008.
[10] G. Adams and P. M. Bubucis, "Calculating an artificial sea water formulation using spreadsheet matrices," Aquarium Sci. Conserv., vol. 2, no. 1, pp. 35–41, 1998, doi: 10.1007/bf00466404.
[11] K. Jamal, M. A. Khan, and M. Kamil, "Mathematical modeling of reverse osmosis systems," Desalination, vol. 160, no. 1, pp. 29–42, Jan. 2004, doi: 10.1016/S0011-9164(04)90015-X.
[12] M. A. Al-Obaidi, A. A. Alsarayreh, A. M. Al-Hroub, S. Alsadaie, and I. M. Mujtaba, "Performance analysis of a medium-sized industrial reverse osmosis brackish water desalination plant," Desalination, vol. 443, pp. 272–284, Oct. 2018, doi: 10.1016/J.DESAL.2018.06.010.
[13] M. Binns, "Analytical models for seawater and boron removal through reverse osmosis," Sustainability (Switzerland), vol. 13, no. 16. 2021. doi: 10.3390/su13168999.
[14] M. A. Al-Obaidi, A. A. Alsarayreh, A. Bdour, S. H. Jassam, F. L. Rashid, and I. M. Mujtaba, "Simulation and optimisation of a medium scale reverse osmosis brackish water desalination system under variable feed quality: Energy saving and maintenance opportunity," Desalination, vol. 565, p. 116831, Nov. 2023, doi: 10.1016/J.DESAL.2023.116831.
[15] E. A. Mason and H. K. Lonsdale, "Statistical-mechanical theory of membrane transport," J. Memb. Sci., vol. 51, no. 1–2, pp. 1–81, Jul. 1990, doi: 10.1016/S0376-7388(00)80894-7.
[16] D. J. Olver and J. D. Benson, "Meta-analysis of the Boyle van 't Hoff relation: Turgor and leak models explain non-ideal volume equilibrium," Cryobiology, vol. 113, p. 104581, Dec. 2023, doi: 10.1016/J.CRYOBIOL.2023.104581.
[17] S. Kimura, "Analysis of reverse osmosis membrane behaviors in a long-term verification test," Desalination, vol. 100, no. 1–3, pp. 77–84, Jan. 1995, doi: 10.1016/0011-9164(96)00009-4.
[18] D. E. Wiley, C. J. D. Fell, and A. G. Fane, "Optimisation of membrane module design for brackish water desalination," Desalination, vol. 52, no. 3, pp. 249–265, Jan. 1985, doi: 10.1016/0011-9164(85)80036-9.
[19] X. Chen, C. Boo, and N. Y. Yip, "Transport and structural properties of osmotic membranes in high-salinity desalination using cascading osmotically mediated reverse osmosis," Desalination, vol. 479, p. 114335, Apr. 2020, doi: 10.1016/J.DESAL.2020.114335.
[20] S. Sundaramoorthy, G. Srinivasan, and D. V. R. Murthy, "An analytical model for spiral wound reverse osmosis membrane modules: Part I —

Journal of Engineering Research (ERJ)
Vol. 7 – No. 3, 2023
©Tanta University, Faculty of Engineering
ISSN: 2356-9441 https://erjeng.journals.ekb.eg/ e ISSN: 2735-4873

Model development and parameter estimation," Desalination, vol. 280, no. 1–3, pp. 403–411, Oct. 2011, doi: 10.1016/J.DESAL.2011.03.047.

[21] V. Gekas and B. Hallström, "Mass transfer in the membrane concentration polarization layer under turbulent cross flow : I. Critical literature review and adaptation of existing sherwood correlations to membrane operations," J. Memb. Sci., vol. 30, no. 2, pp. 153–170, Feb. 1987, doi: 10.1016/S0376-7388(00)81349-6.

[22] J. I. H. Philip M. Gerhart, Andrew L. Gerhart, Fundamentals of Fluid Mechanic, 8th Edition. 2016.

[23] Holman, J. P. (Jack Philip) Experimental methods for engineers / J.P. Holman. -8th ed. p. cm.- (McGraw-Hill series in mechanical engineering).

Doi: 10.21608/ERJENG.2023.234375.1230